Computational NMR Spectroscopy of Transition-Metal/Nitroimidazole Complexes: Theoretical Investigation of Potential Radiosensitizers

by **Teodorico C. Ramalho**[a]), **Michael Bühl***[b]), **José Daniel Figueroa-Villar**[a]), and **Ricardo Bicca de Alencastro**[c])

[a]) Departamento de Química, Instituto Militar de Engenharia, 22290-270 Rio de Janeiro, RJ, Brazil
[b]) *Max Planck*-Institut für Kohlenforschung, Kaiser-Wilhelm-Platz 1, D-45470 Mülheim an der Ruhr, Germany
[c]) Grupo de Físico-Química Orgânica, Departamento de Química Orgânica, Instituto de Química, Universidade Federal do Rio de Janeiro, Ilha do Fundão, CT, Bl. A, Lab. 609, 21949-900, Rio de Janeiro-RJ, Brazil

The computed chemical shifts of transition-metal complexes with dimetridazole (=1,2-dimethyl-5-nitro-1*H*-imidazole; **1**), a prototypical nitro-imidazole-based radiosensitizer, are reported at the GIAO-BP86 and -B3LYP levels for BP86/ECP1-optimized geometries. These complexes comprise $[MCl_2(\mathbf{1})_2]$ (M = Zn, Pd, Pt), $[RuCl_2(DMSO)_2(\mathbf{1})_2]$, and $[Rh_2(O_2CMe)_4(\mathbf{1})_2]$. Available $\delta(^1H)$ and $\delta(^{15}N)$ values, and $\Delta\delta(^1H)$ and $\Delta\delta(^{15}N)$ coordination shifts are well-reproduced theoretically, provided solvation and relativistic effects are taken into account by means of a polarizable continuum model and suitable methods including spin–orbit (SO) coupling, respectively. These effects are particularly important for the metal-coordinated N-atom, where the contributions from solvation and relativity can affect $\delta(^{15}N)$ and $\Delta\delta(^{15}N)$ values up to 10–20 ppm. The ^{195}Pt chemical shifts of *cis*- and *trans*-$[PtCl_2(\mathbf{1})_2]$ are well-reproduced using the zero-order regular approximation including SO coupling (ZORA-SO). Predictions are reported for ^{99}Ru and ^{103}Rh chemical shifts, which suggest that these metal centers could be used as additional, sensitive NMR probes in their complexes with nitro-imidazoles.

1. Introduction. – NMR Spectroscopy is one of the most important methods for the characterization of electronic and structural properties of molecules [1–3]. Experimental spectra can often be successfully interpreted empirically, but more difficult cases can benefit from predictions based on electronic-structure calculations. In the past 25 years, the computation of magnetic-resonance parameters from first principles has become a powerful research tool that can significantly enhance the utility of magnetic resonance techniques [4][5]. This is particularly true for inorganic or organometallic species, where empirical interpretations are far more difficult [5][6].

In this context, metal complexes of nitro-1*H*-imidazoles are of special interest due to their chemical and pharmacological properties [7]. It is known that their biological activity is rooted in the interaction with DNA, and the formation of free radicals involving the N_2 group must play an important role in the mechanism of action [7][8]. This property makes nitro-imidazoles and their derivatives the most commonly used radiosensitizers of hypoxic cells [7][8], *e.g.*, compounds **1**–**4** and their complexes with metals like ^{195}Pt and ^{99}Ru [9]. Because the first nitro-1*H*-imidazole drugs such as metronidazole (=methyl-5-nitro-1*H*-imidazol-1-ethanol; **2**) exhibited many undesired side effects, there is much ongoing research in this area, including studies on bioreducible groups other than N_2 [10–12]. Ruthenium and platinum complexes with **2** have been used as chemotherapeutic agents [13][14], while a ^{99m}Tc nitro-1*H*-imidazole complex has been used as hypoxic marker in myocardial and cerebral ischemia [15]. Recently, ^1H-, ^{31}P-, and ^{19}F-NMR/MRI (Magnetic Resonance Imaging) [16] of nitro-1*H*-imida-

zoles has been applied for measuring tumor [17] and tissue oxygenation [18]. 1-[2-(Ethylsulfonyl)ethyl]-2-methyl-5-nitro-1*H*-imidazole (**4**) labeled with ^{3}H showed localized accumulation in patients, and other nitro-1*H*-imidazoles labeled with ^{19}F or ^{123}I have been investigated as possible non-invasive markers of hypoxia [17][19][20]. However, these non-invasive compounds are not widely applicable because of the need for expensive isotopes and special chemical syntheses [20]. The synthesis of metal complexes of unlabeled nitro-1*H*-imidazoles offered the possibility of more routine and inexpensive imaging of hypoxia in damaged normal tissue or in tumors [17]. In spite of the great importance of multinuclear NMR spectroscopy for such metal complexes of radiosensitizers, no detailed computational work on this subject has been reported so far.

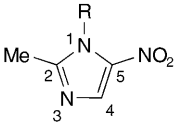

1 R = Me
2 R = $HOCH_2CH_2$
3 R = $MeCH(OH)CH_2$
4 R = $MeCH_2SO_2CH_2CH_2$

In our previous works, we have studied physico-chemical properties associated with biological activity of radiosensitizers in aqueous and CCl_4 solutions [21–25]. Furthermore, we used [23][25] the theoretical approach by *Canuto* and *Coutinho* [26–29]. Recently, we have assessed NMR properties of nitro-1*H*-imidazoles computed with the modern tools of density-functional theory (DFT) [24]. The same tools have been successfully applied to calculate chemical shifts of ligands in the coordination sphere of transition metals, as well as those of the metals themselves [30][31]. These findings are in keeping with the overall good performance of DFT methods for calculating structures and properties of transition metal complexes [30][32][33].

First-principles computation of NMR parameters, either chemical shifts or spin-spin coupling constants, can be very useful for the interpretation of recorded spectra and for investigating structure-property relationships [4][34]. Magnetic shieldings and chemical shifts are known to be 'sensitive to everything' [35]. This sensitivity poses considerable challenges for the quantum-mechanical description of NMR parameters [4]. While accurate chemical shift calculations can now be performed routinely for light nuclei, in particular in first-row compounds [5][36][37], the computational challenges are still substantial in heavy element compounds, and suitable theoretical NMR methods have only very recently become available or are still being developed [35][38]. It is clear that DFT is especially suitable for larger molecules, such as biological systems, because it is an inexpensive computational technique capable of reliably predicting NMR parameters [4][39].

In this communication, we will report the NMR calculation of transition metal complexes of dimetridazole (**1**), calling attention to geometrical, solvent, scalar relativistic, and spin–orbit effects on ^{15}N, ^{1}H, ^{99}Ru, ^{103}Rh and ^{195}Pt chemical shifts by means of modern DFT-based approaches.

2. Methodology. – 2.1. *Geometry Optimization*. Geometries were fully optimized by the gradient-corrected BP86 combination of density functionals [40], Stuttgart–Dresden effective core potentials (ECPs), together with the corresponding valence basis

sets on the metals [41][42] and 6-31G* basis set on the ligands (denoted ECP1). The initial optimization of the complexes started from the coordinates taken from the following solid-state structures: *trans*-[$PdCl_2$(**2**)$_2$] [43], [$RuCl_2(Im)_2(DMSO)_2$] (Im = 1*H*-imidazole) [44], [$ZnCl_2$(**2**)$_2$] [45], [$Rh_2(OAc)_4$(**2**)$_2$] [46], and *cis*- and *trans*-[$PtCl_2$(**2**)$_2$] [47].

2.2. *NMR Calculations.* Magnetic shieldings σ were computed for equilibrium geometries by two approaches.

Method 1. Magnetic shieldings were calculated at the GIAO (gauge-including atomic orbitals) [48] -BP86 and -B3LYP [49] levels employing basis II′ [50] for the ligands (DZ basis [50] on H atoms), and a [16s10p9d] all-electron basis for Ru and Rh, which is contracted from the well-tempered 22s14p12d set of *Huzinaga* and *Klobukowski* [51], and augmented with two d-shells of the well-tempered series. For Pt, Zn, and Pd the Stuttgart–Dresden ECPs were employed. Shieldings were either evaluated *in vacuo* or in the presence of a polarizable continuum in the integral equation formalism model [52–55], using the dielectric constants of H_2O. Previous studies have shown that this combination gave a good agreement between theory and experiment for a number of test cases [24][56][57]. These (non-relativistic) NMR calculations were carried out with Gaussian03 [58].

Method 2. Additional NMR calculations were performed with the Amsterdam density-functional code ADF [59–61] employing the BP86 functional [40]. This functional is a well-established and reliable GGA that has been successfully applied in many NMR computations involving heavy elements [38][39]. The two-component relativistic 'zeroth-order regular approximation' (ZORA) [62] density-functional (DFT) method including scalar and spin–orbit (SO) [63] corrections has been employed for the computations. We have used two different all-electron *Slater*-type basis sets in order to assess the dependence of the results on the quality of the basis. The first one is a triple-ξ basis set plus one polarization functions for all atoms (denoted TZP). The second is a mixed one employing TZP for just N and metal atoms, and a polarized double-ξ basis on the remainder of the complex (denoted TZP′).

For pristine **1**, ^{15}N- and ^{1}H-NMR chemical shifts δ have been calculated relative to $MeNO_2$ and benzene, respectively, optimized or simulated at the same level (no bulk solvent effects using PCM methods were evaluated for these reference compounds, as they are used in neat form experimentally, rather than dissolved in a polar solvent). The corresponding σ values are collected in *Table 1*. The resulting ^{1}H-NMR chemical shifts were converted to the usual TMS (Me_4Si) scale, using the experimental value for benzene of $\delta(^{1}H) = 7.26$ ppm [64]. The ^{15}N- and ^{1}H-chemical shifts of **1** are collected in *Table 2,* together with experimental data [65][66]. For the metal complexes **5**–**12**, coordination shifts are reported, *i.e.*, the difference $\Delta\delta$ with respect to the data in *Table 2*, computed at the same level. ^{195}Pt and ^{99}Ru chemical shifts δ have been calculated relative to cisplatin (= *cis*-[$PtCl_2(NH_3)_2$]) and RuO_4, respectively, because the experimental standards of 1M (or saturated) aqueous solution of both [$K_4Pt(CN)_6$] and [$K_4Ru(CN)_6$] are difficult to model theoretically [31]. The resulting chemical shifts were converted to the usual δ scales using the experimental value for cisplatin and RuO_4, *i.e.*, $\delta(^{195}Pt) -2100$ [67] and $\delta(^{99}Ru)$ 1976 ppm (mean value from [68]), respectively.

Table 1. *Magnetic Shielding Constants for Reference Compounds Computed at Various Levels.* The pertinent atoms are highlighted in italics. The calculations employed BP86/ECP1 geometries [a]).

Compound	BP86/II′	B3LYP/II′	NREL/TZP	ZORA/TZP′	ZORA-SO/TZP′
$CH_3\mathit{N}O_2$	– 132.6	– 168.4	– 138.8	– 133.9	– 132.3
$C_6\mathit{H}_6$	24.4	24.6	24.0	24.0	24.2
$\mathit{Ru}O_4$	– 2518	– 3094	– 1752	– 1601	– 1645
cis-[$\mathit{Pt}Cl_2(NH_3)_2$]	–	–	2118	2958	3236

[a]) II′ and TZP′ results obtained with Gaussian03 and ADF programs, respectively.

Table 2. *Computed ^{15}N- and ^{1}H-NMR Chemical Shifts* (in ppm) *of Pristine Dimetridazol* **1**

Level[a])	N(3)	N(1)	H–C(4)	Me–C(1)[b])	Me–C(2)[b])
BP86/II′	– 88.6	– 204.5	7.7	3.6	2.3
B3LYP/II′	– 116.6	– 239.3	7.9	3.7	2.4
BP86/PCM/II′[c])	– 100.3	– 199.1	8.0	3.7	2.4
B3LYP/PCM/II′[c])	– 129.6	– 233.9	8.2	3.8	2.5
NREL/TZP	– 91.8	– 207.5	7.7	3.5	2.1
ZORA/TZP′	– 88.2	– 203.5	7.6	3.7	2.4
ZORA-SO/TZP′	– 86.7	– 201.9	7.6	3.7	2.4
Experiment[d])	*– 121.0*	*– 224.1*	*7.9*	*3.9*	*2.5*

[a]) BP86/AE1 Geometry employed. [b]) $\delta(^1H)$ Values. [c]) Employing a polarizable continuum with the dielectric constant of H_2O. [d]) Experimental ^{15}N and ^{1}H data from [65] and [66], respectively.

For $\delta(^{103}Rh)$, due to the lack of a suitable reference compound, the magnetic-shielding values corresponding to $\delta(^{103}Rh)$ are reported relative to σ(standard) = – 878 ppm, as previously evaluated from a linear regression of σ(calc.) *vs.* δ(exper.) at the B3LYP level [69].

3. Results and Discussion. – Among the nitro-1*H*-imdazole derivatives, dimetridazole (= 1,2-dimethyl-5-nitro-1*H*-imidazole; **1**) and its complexes **5**–**12** with the d-block elements Zn, Ru, Rh, Pd, and Pt are prototypical representatives (*Fig. 1*). Some of them have been used in the treatment of anaerobic protozoan and bacterial infections [7] [8]. We have, thus, chosen these species as targets for extensive test of the computational methodologies available for computation of NMR properties, calling special attention to the electronic and structural effect on ^{15}N- and ^{1}H-NMR chemical shifts, which are widely used for the characterization of such complexes. In this study, we will extend the first-principle calculation of NMR parameters from lighter (Zn) to the heavier part of the periodic table (Pt), *i.e.*, to d-block compounds using nitro-1*H*-imidazole complexes of biological interest, both in the gas phase and solution. The complexes **5**–**12** cover different coordination geometries (tetrahedral, octahedral, square-planar), and are structurally well-characterized, the actual solid-state structures of the complexes with ligand **1** (or, alternatively, with ligand **2** or with Im) being known. For the octahedral and square planar species, isomeric complexes have been considered, *i.e.*, for the pairs **6**/**7**, **9**/**10**, and **11**/**12**, following precedence in the literature for corresponding isomerism.

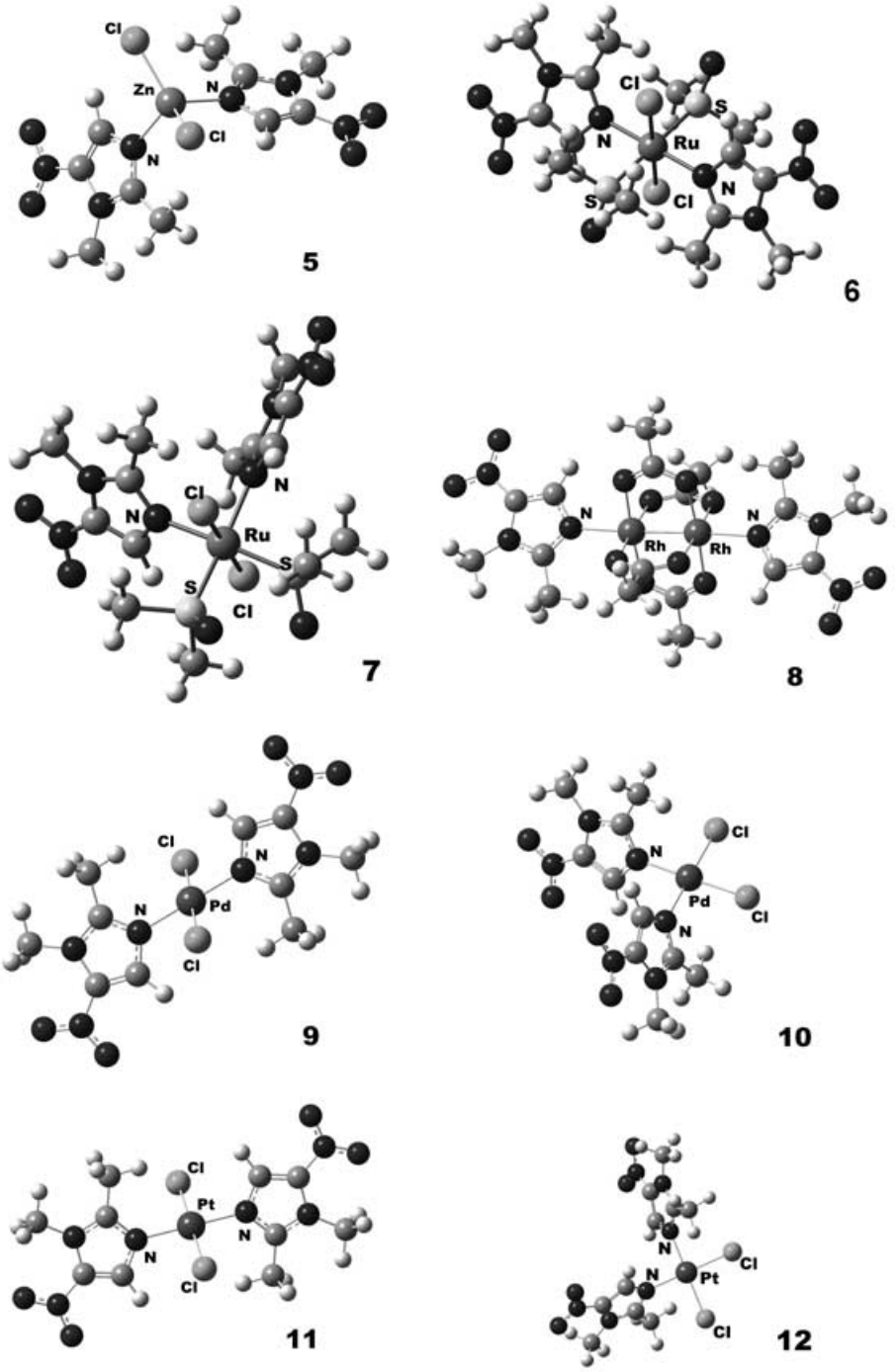

Fig. 1. *Optimized structures of the metal complexes* **5**–**12** *with dimetridazole* (**1**). Constitutions: $[ZnCl_2(\mathbf{1})_2]$ (**5**), $[RuCl_2(DMSO)_2(\mathbf{1})_2]$ (**6**/**7**), $Rh(OAc)_4(\mathbf{1})2]$ (**8**), $[PdCl_2(\mathbf{1})_2]$ (**9**/**10**), and $[PtCl_2(\mathbf{1})_2]$ (**11**/**12**).

The choice of metal centers has in part been motivated by their potential use as additional NMR probe. In particular, ^{99}Ru, ^{103}Rh, and ^{195}Pt are fairly well-behaved NMR nuclei, for which sizeable amounts of data are available [2]. Interest in ^{99}Ru-NMR spectroscopy has recently been renewed, both from experimental [70] and computational viewpoints [31][71]. Several research groups have investigated the possibility of employing ^{103}Rh-NMR spectroscopy as a probe to detect the thermodynamic stability of bimetallic complexes and predict their catalytic activity [72][73]. The ^{195}Pt-NMR nucleus is a popular probe for the electronic and geometrical structures of Pt complexes and can be used to study, for instance, the coordination behavior of imidazole moieties to Pt^{II} in order to understand the mechanism of interaction of Pt drugs with histidyl-imidazole N-atoms in proteins [74]. In addition, ^{195}Pt-NMR spectroscopy has widely been used to investigate the structure–activity relation in complexes of biological interest [74][75]. The Zn complex **5** has been selected to provide some structural variety (tetrahedral coordination geometry), and the Pd species **9**/**10** for comparison with the Pt congeners **11**/**12**.

This section is organized as follows: first, chemical shifts from non-relativistic gas-phase calculations are discussed (*Sect. 3.1*), followed by evaluation of solvent effects (*Sect. 3.2*). Finally, relativistic effects, in particular due to spin–orbit (SO) coupling, are addressed (*Sect. 3.3*).

3.1 *Non-Relativistic Chemical Shifts in the Gas Phase.* For the complexes of this study, ^{1}H-NMR spectroscopy has so far been the usual means of characterization, and no ^{13}C-NMR data have been reported yet. Experimental $\delta(^{15}N)$ data are sparse, but are known for both isomers **11**/**12** [66]. Referencing ^{15}N chemical shifts is a notorious problem [76][77]; due to inconsistencies between the $\delta(^{15}N)$ values reported for pristine **1** in [66] and those reported previously for the same compound [65], or for related nitro-1*H*-imidazoles [24], we decided to present the ^{15}N and ^{1}H data for the metal compounds as complexation shifts, *i.e.*, as $\Delta\delta$ values relative to the data for the free ligand in *Table 2*. Calculated and, where available, observed ^{15}N and ^{1}H coordination shifts are collected in *Table 3*. For these light nuclei, results obtained with BP86 and B3LYP functionals are fairly similar. Most H-atoms and N(1) are deshielded by up to *ca.* 1–7 ppm, respectively, and the corresponding experimental data for **11** and **12** are reasonably well reproduced. The coordinating N-atom, N(3), is strongly shielded throughout, between *ca.* −25 and −70 ppm. Here, the experimental data for **11** and **12** are less well captured, and the observed shieldings exceeding −100 ppm are significantly underestimated, by *ca.* 40 ppm. As will be shown in *Sect. 3.3*, a large part of this discrepancy is due to relativistic effects, which are particularly important for this nucleus, since it is directly attached to a heavy element, Pt.

Relativistic effects are known to strongly influence the chemical shifts of 5d elements such as ^{195}Pt [62][78]. Therefore, we did not calculate $\delta(^{195}Pt)$ values using the non-relativistic method (see *Method 1* in the *Methodology*; for relativistic values, see *Sect. 3.3*). In contrast, observed $\delta(^{103}Rh)$ and $\delta(^{99}Ru)$ values have been well reproduced computationally at non-relativistic levels for larger sets of compounds (at the B3LYP/II′ level using BP86/ECP1 geometries) [31][39][69]. The δ(metal) values for the Ru and Rh complexes **6**–**8** (*Table 3*), obtained at the same level, should thus be reliable predictions, with possible error margins of just a few hundred ppm, *i.e.*, a few percent of the respective chemical-shift range of the metal.

Table 3. *Computed ^{15}N- and ^{1}H-NMR Non-Relativistic Gas-Phase Coordination Shifts $\Delta\delta$* (in ppm) *for Complexes* **5**–**12**. Selected metal chemical shifts are also given.

Compound	Level[a])	N(3)	N(1)	H–C(4)	Me–C(1)[b])	Me–C(2)[b])	Metal
5	BP86	−41.8	4.7	0.8	0.3	0.4	–
	B3LYP	−44.3	4.3	1.1	−0.1	0.4	
6	BP86	−40.2	5.1	1.0	0.1	0.6	4673[c])
	B3LYP	−46.1	6.7	1.2	0.1	0.5	5713[c])
7	BP86	−34.6	4.1	0.9	−0.1	−0.1	4638[c])
	B3LYP	−38.1	5.2	1.0	−0.2	−0.1	5650[c])
8	BP86	−21.1	1.0	0.9	0.3	0.5	–
	B3LYP	−24.6	1.1	1.0	0.4	0.5	7917[d])
9	BP86	−63.8	1.6	0.2	0.2	0.6	–
	B3LYP	−67.8	1.8	0.3	0.2	0.6	
10	BP86	−59.7	3.0	−0.0	0.6	0.1	–
	B3LYP	−61.2	3.1	−0.5	0.8	0.2	
11	BP86	−57.1	1.6	0.2	0.4	0.3	–
	B3LYP	−62.2	2.9	0.3	0.3	0.1	
	Exper.	*−108.5*	*3.1*	*0.1*	*0.2*	*0.5*	*−2061*[e])
12	BP86	−53.1	2.9	0.5	0.5	0.3	–
	B3LYP	−57.0	4.5	0.4	0.1	0.4	
	Exper.	*−100.1*	*3.8*	*0.4*	*0.1*	*0.5*	*−2069*[e])

[a]) Functional in NMR computation; basis II′ and BP86/ECP1 geometries were employed throughout. [b]) $\Delta\delta(^{1}H)$ values. [c]) $\delta(^{99}Ru)$. [d]) $\delta(^{103}Rh)$. [e]) $\delta(^{195}Pt)$.

In fact, the ^{103}Rh chemical shifts of compounds closely related to **8** are known [79][80]. For instance, for $[Rh_2(OAc)_4\{P(OMe)_3\}_2]$ (**13**), a $\delta(^{103}Rh)$ value of 6694 ppm has been reported [79]. This value is not too far from the one predicted for **8** (*ca.* 7900 ppm, *Table 3*). We have also computed $\delta(^{103}Rh)$ of complex **13** (see *Fig. 2* for a plot of the optimized structure, where we imposed C_2 symmetry and adopted a conformation of the $P(OMe)_3$ ligand as that found in the solid for the related $P(OPh)_3$ complex [81]). At the B3LYP/II′ level, a δ value of 7060 ppm is obtained for **13**, which is slightly too deshielded with respect to experiment, but still with an acceptable accuracy. Apparently, no serious degradation of the B3LYP data is found for compounds containing Rh,Rh multiple bonds, in contrast to Mo,Mo multiply bonded systems [82]. Replacement of the phosphine ligands in **13** by nitro-1*H*-imidazoles, thus, results in a significant deshielding of the metal (by *ca.* 800–900 ppm). Since ^{103}Rh chemical shifts have proven to be a sensitive analytical tool for compounds with a $[Rh_2(O_2CR)_4]$ core [80], compound **8** and other nitro-1*H*-imidazole derivatives could also be attractive targets for ^{103}Rh-NMR spectroscopy.

Quadrupolar line broadening can be a serious impediment for ^{99}Ru-NMR spectroscopy, and the metal in complexes **6** and **7** with their rather unsymmetrical ligand environment may be difficult to detect. Highly symmetrical hexakis(1*H*-imidazole) ruthenium(II) salts are known [83], but, to our knowledge, no hexakis(nitro-1*H*-imidazole) complexes have been reported (for a 5-nitro-1*H*-imidazole derivative in the solid, see [84]. Due to the expected low electric field gradient (EFG) at the metal, these complexes should be readily amenable to ^{99}Ru-NMR spectroscopy. For future reference, we note the predicted (B3LYP/II′ level) $\delta(^{99}Ru)$ values of 6531 and 10191 ppm for

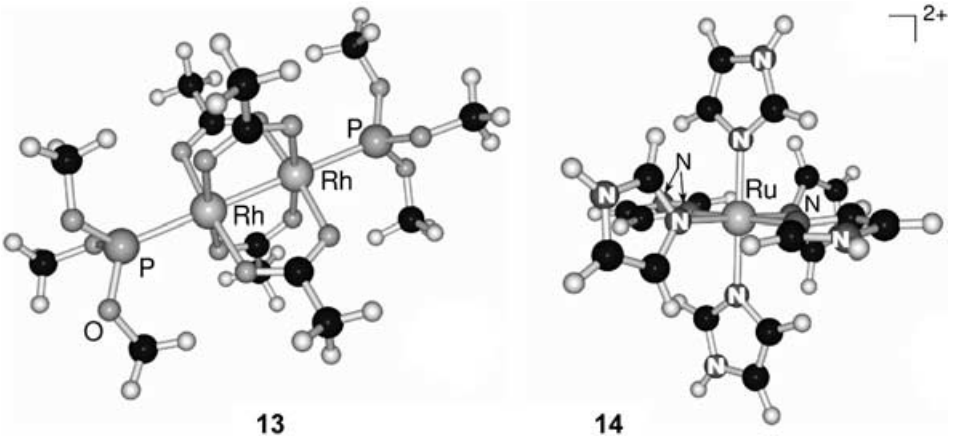

Fig. 2. *Structures of the complexes* **13** *and* **14** (BP86/ECP1 optimized). The two compounds are structurally related to complexes **8** and **7**, respectively.

$[Ru(Im)_6]^{2+}$ (**14**) and $[Ru(\mathbf{1})_6]^{2+}$ (not shown), respectively, both optimized in S_6 symmetry (see *Fig. 2* for the optimized structure of **14**).[1])

Due to unfavorable NMR properties of all Zn isotopes, NMR resonances of this metal have been observed only sparingly [2], and the eventual development of Zn-NMR spectroscopy into an analytical tool is not quite foreseeable at this point. Hence, we have not calculated relative Zn chemical shifts for **5**, which was selected for its coordination geometry, rather than for its use in metal NMR. The same is true for the Pd complexes **9** and **10**, which were included for comparison with the Pt congeners **11** and **12**.

To test if part of the deviations for N(3) could be due to shortcomings in the optimized geometries, we have assessed the specific effect of the corresponding metal–N bond length by calculating the magnetic shielding constants of each complex, fixing the metal–N bond lengths to those from the corresponding X-ray structures, and leaving all other parameters at their optimized values. The BP86 metal–N(3) bond lengths in the gas phase tend to be longer than those observed in the solid, namely by *ca*. 0.056, 0.087, 0.013, 0.029, and 0.028 Å for the complexes **5**, **7**, **8**, **9**, and **11**, respectively (*Table 4*). This increase in bond distance results in a deshielding of the N(3)-atom by 5.2, 0.9, 2.7, 0.8, and 1.8 ppm in the complexes **5**, **7**, **8**, **9**, and **11**, respectively, and corresponds to bond-length/shielding derivatives $\partial\sigma^{N(3)}/\partial r$ of -92.8, -10.3, -207.7, -27.9, and -64.3 ppm/Å for **5**, **7**, **8**, **9**, and **11**, respectively. Thus, geometrical effects on $\delta(N(3))$ values are noticeable, but are much too small to contribute significantly to the large deviations encountered in the non-relativistic calculations.

The computed bond-length/shielding derivative for ^{99}Ru and ^{103}Rh (by *Method 1*; see *Methodology*) is $\partial\sigma^{Ru}/\partial r = -8232$ and $\partial\sigma^{Rh}/\partial r = 9582$ ppm/Å in complexes **7** and

---

[1]) The huge deshielding of the ^{99}Ru nucleus in $[Ru(\mathbf{1})_6]^{2+}$ is related to the very long Ru–N bonds, 2.195 Å at BP86/ECP1, by more than 8 pm longer than those in **14**, 2.113 Å at the same level (average value in the solid: 2.099 Å [83a]). The steric encumbrance in $[Ru(\mathbf{1})_6]^{2+}$ makes its eventual preparation quite unlikely.

Table 4. *Optimized* vs. *Experimental Bond Distances* (in Å) *for Complexes* **5**–**12**

Compound	Distance	Experiment [43–47]	Optimized (BP86/ECP1)
5	Zn–N	2.044	2.100
	Zn–Cl	2.238	2.301
6	Ru–N	–	2.123
	Ru–Cl	–	2.450
	Ru–S	–	2.326
7	Ru–N	2.104	2.191[a])
	Ru–Cl	2.416	2.450
	Ru–S	2.289	2.285
8	Rh–N	2.240	2.253
	Rh–Rh	2.446	2.389
9	Pd–N	2.007	2.036
	Pd–Cl	2.297	2.342
10	Pd–N	–	2.074
	Pd–Cl	–	2.310
11	Pt–N	2.000	2.032
	Pt–Cl	2.363	2.296
12	Pt–N	–	2.057
	Pt–Cl	–	2.331

[a]) 2.157 Å in the complex with 1*H*-imidazole, to which the X-ray value refers.

8, respectively. As expected, the $\partial\sigma$(metal)/∂r values are much larger than $\partial\sigma$(N(3))/∂r, reflecting the much larger chemical-shift ranges of the metals [2]. In addition, the chemical shift of the metal can be mildly sensitive to conformational changes (see, *e.g.*, the metal entries for **6** and **7** in *Table 3*). Very likely, this sensitivity of the metal chemical shifts to geometrical parameters entails a noticeable importance of zero-point or thermal corrections. Due to the substantial computational expense, we have not included such corrections for the complexes of this study, which can be evaluated using perturbational or molecular dynamics approaches [85][86].

3.2. *Solvent Effects.* Most chemical and biochemical processes take place in solution, which may strongly affect reactivities and properties. Solvent effects on molecular properties can be classified as *direct* or *indirect* [24]. The direct effects, on the one hand, are due to specific, usually short-range interactions between solvent and solute, and to the concomitant response of the electronic wavefunction of the latter. The indirect effects, on the other hand, arise from the changes in molecular geometry caused by the presence of the solvent. Both effects on chemical shifts can be sizeable, in particular for protic and polar solvents such as H_2O or MeCN, in which the experimental spectra for **11**/**12** [66] were recorded (*Table 3*).

In our previous study of metronidazole (**2**), we have shown that a simple continuum approach can qualitatively reproduce both direct and indirect solvent effects on NMR properties [24]. Furthermore, recent studies [87][88] have shown that treating the solvent implicitly as a polarizable continuum may yield important contributions to the NMR parameters. In line with these observations, we have chosen the PCM methodology to analyze the solvent effects. The PCM method can be applied at two stages, first in the geometry optimization, and second, during the evaluation of the magnetic shielding constants. For the ligand nuclei, indirect solvent effects turn out to be relatively small in

magnitude, consistent with our previous observation that geometrical effects are of lesser importance for the complexes studied. It is well-known that the cavity definition in continuum solvation methods can have a large impact on the computed properties [56]. In the PCM approach we applied, the cavity is defined as an envelope of spheres centered on atoms with radii of these spheres equal to the *Van der Waals* radii scaled by the standard value of 1.2.

To evaluate the direct solvation effect, we applied the PCM method with the geometries optimized *in vacuo*. As expected, the computed values are very similar when the dielectric constants of H_2O and MeCN, the solvents used experimentally, are employed, and only the values for H_2O are given in *Tables 2* and *5*. For the free ligand **1**, the N(3) chemical shift is systematically shielded in solution, by *ca*. 12 and 13 ppm at BP86 and B3LYP levels, respectively (compare corresponding II′ and PCM/II′ entries in *Table 2*), consistent with previous results for compound **2** [24]. For the metal complexes **5**–**12**, N(3) is usually shielded upon solvation, too, but either to a lesser or to a larger extent, so that the solvent effect on the coordination shifts is rather unsystematic (compare corresponding entries in *Tables 3* and *5*). The estimated solvent effect on the coordination shift $\Delta\delta(^{15}N)$ for N(3) amounts to +2.2 and +0.1 ppm for **11** and **12**, respectively (BP86 data), which does not reduce the deviation from experiment. For the ^{1}H nuclei, much smaller solvent effects on the coordination shifts are computed, which rarely exceed 0.2 ppm (*Table 4*). In summary, solvation effects can affect the chemical shifts themselves (see *Table 2*), but tend to be of lesser importance for the coordination shifts upon complexation (compare *Tables 3* and *5*).

According to the data in *Table 5*, the ^{99}Ru nuclei in **6** and **7** are deshielded upon solvation, by up to *ca*. 200 ppm (B3LYP for **6**), while the ^{103}Rh nucleus in **8** is shielded by *ca*. 400 ppm. Unfortunately, there are no experimental data for comparison.

Table 5. *Computed Coordination Shifts* (in ppm, II′ basis) *for Complexes* **5**–**12** *Including Bulk Solvation Effects Modeled by a Polarizable Continuum* (parameters for water employed)

Compounds	Level[a])	N(3)	N(1)	4-H	1-Me[a])	2-Me[a])	Metal
5	BP86	−37.1	10.2	0.4	0.2	0.3	–
	B3LYP	−38.9	6.2	0.4	0.2	0.5	
6	BP86	−34.1	6.7	0.6	0.2	0.5	4827[b])
	B3LYP	−40.6	8.4	0.7	0.2	0.4	5918[b])
7	BP86	−31.9	5.6	0.4	0.0	−0.2	4742[b])
	B3LYP	−36.8	6.9	0.8	0.0	−0.2	5820[b])
8	BP86	−27.2	2.1	0.8	0.3	0.4	–
	B3LYP	−29.6	3.1	0.8	0.2	0.3	7521[c])
9	BP86	−48.8	3.9	0.3	0.3	0.5	–
	B3LYP	−52.2	4.8	0.5	0.2	0.7	
10	BP86	−44.5	3.7	0.3	0.2	0.1	–
	B3LYP	−47.9	5.8	0.3	0.1	0.1	
11	BP86	−54.9	3.5	0.2	0.2	0.1	–
	B3LYP	−62.5	2.6	0.2	0.2	0.1	
12	BP86	−53.0	4.4	0.0	0.2	0.0	–
	B3LYP	−61.0	5.9	0.1	0.2	0.1	

[a]) $\Delta\delta(^{1}H)$. [b]) $\delta(^{99}Ru)$. [c]) $\delta(^{103}Rh)$.

3.3. *Scalar Relativistic and Spin-Orbit Effects.* Proper treatment of relativistic effects in the calculation of molecular properties is an active area of research [4]. We have used the popular ZORA approach (as implemented in the ADF program and together with the BP86 functional), which has been shown to hold great promise for NMR properties of heavy elements [38]. Other methods of including relativistic effects into NMR shielding calculation have been proposed in the literature, for instance, using variational or perturbational *Pauli* schemes, and/or suitable ECPs at the heavy nuclei [89][90]. In particular, DFT-ECP calculations have been performed successfully for the chemical shifts of ligand nuclei in the coordination sphere of transition metals [30][89][90]. What makes ZORA very attractive based on theoretical grounds is that it avoids rather than circumvents the fundamental stability problems of the *Pauli* operator [62].

It is well-known that scalar and often SO relativistic effects have to be included for even a qualitative understanding of the chemical shifts in systems containing heavy elements [50]. In particular, δ values for lighter NMR nuclei bonded to such heavy elements can be strongly affected by SO coupling, according to a *Fermi*-contact mechanism, which is now well understood (see, *e.g.*, [91]).

Calculated NMR shieldings can be very sensitive to the size of the basis set, even with a distributed-gauge method like GIAO. In first orienting calculations for cisplatin, we have tested two *Slater*-type basis sets, one of TZP quality on all atoms, and a locally dense one with TZP basis just on N- and metal atoms, and DZP basis on the remainder (denoted TZP′). As can be seen from the data in *Table 6*, there are only minor differences in the ^{15}N shifts and ^{195}Pt shieldings with these two basis sets. On going from the full TZP basis to TZP′, the ZORA and ZORA-SO results differ by just *ca.* 6 ppm for $\delta(^{15}\text{N})$, and by 44 and 34 ppm, respectively, for $\delta(^{195}\text{Pt})$. As these are relatively minor differences, we have employed the mixed TZP′ basis for all further ZORA calculations due to its lower computational cost.

Table 6. *Calculated ^{15}N-NMR Chemical Shifts and ^{195}Pt Shielding Constants* (in ppm) *for Cisplatin* (*cis*-$[PtCl_2(NH_3)_2]$) *with Different Basis Sets* (see *Methodology*)

Method	TZP		TZP′	
	$\delta(^{15}\text{N})$	$\sigma(^{195}\text{Pt})$	$\delta(^{15}\text{N})$	$\sigma(^{195}\text{Pt})$
NREL	−387.8	2118	–	–
ZORA	−371.9	3002	−365.9	2958
ZORA-SO	−390.3	3270	−384.2	3236
δ(*exper.*)	*−426.8*[a])	–	–	–

[a]) From [67] (converted from the NH_4NO_3/HNO_3 to the $MeNO_2$ scale with a conversion factor of −359.0 ppm [76]).

For the complexes of this study, scalar relativistic effects are small for N nuclei (*ca.* 2–3 ppm; compare ZORA and NREL values in *Table 7*). Similar results are obtained for **5**–**10**, when, in the non-relativistic BP86/II′ (or B3LYP/II′) calculations (see *Table 2*), the all-electron basis on the metal is replaced by a relativistically adjusted ECP. Likewise, fairly small scalar relativistic effects are found for the metal shifts, *ca.* 17–30 ppm (*Table 7*). SO Effects on N(3), as expected, increase from **5** to **12** (compare

Table 7. *Computed ^{15}N-NMR Coordination Shifts and Metal Chemical Shifts at Non-Relativistic, ZORA, and ZORA-SO Levels* (in ppm)[a])

Complex	Method	N(3)	N(1)	Metal
5	NREL	−41.9	4.0	–
	ZORA	−42.3	4.7	–
	ZORA-SO	−41.9	4.8	–
6	NREL	−39.5	4.7	4277[b])
	ZORA	−39.2	3.1	4111[b])
	ZORA-SO	−56.6	2.3	4014[b])
7	NREL	−35.8	3.8	4211[b])
	ZORA	−35.4	2.3	4116[b])
	ZORA-SO	−47.8	1.9	4018[b])
9	NREL	−55.7	3.1	–
	ZORA	−57.3	2.5	–
	ZORA-SO	−70.7	3.6	–
10	NREL	−51.5	4.5	–
	ZORA	−50.8	3.9	–
	ZORA-SO	−59.3	3.9	–
11	NREL	−57.2	3.1	−1963[c])
	ZORA	−53.1	1.1	−2024[c])
	ZORA-SO	−75.3	0.5	−2068[c])
	Exper.	*−108.5*	*3.1*	*−2061*[c])
12	NREL	−50.9	4.2	−1984[c])
	ZORA	−50.7	2.5	−2054[c])
	ZORA-SO	−64.6	2.6	−2104[c])
	Exper.	*−100.1*	*3.8*	*−2069*[c])

[a]) TZP basis for NREL, and TZP′ basis for ZORA and ZORA-SO levels. [b]) $\delta(^{99}\text{Ru})$. [c]) $\delta(^{195}\text{Pt})$.

ZORA-SO and ZORA values in *Table 7*). For instance, the SO effect is just 0.4 ppm in complex **5**, whereas it is *ca*. 8–16 ppm for the complexes from **6**–**10**, and up to 22 ppm in **11**. SO Effects on N(1) are invariably small, up to *ca*. 2 ppm. Interestingly, the ^{15}N(3) signal can be quite strongly influenced by SO effects in the 4d complexes (*e.g.*, for **6** and **9**). For $\delta(^{99}\text{Ru})$, the effect of SO coupling affords an increased shielding, by about −100 ppm for complexes **6** and **7**. For $\delta(^{195}\text{Pt})$ in **11** and **12**, SO effects are also shielding, between *ca.* −60 and −80 ppm. Relative to the large ^{195}Pt chemical-shift range, these effects are quite small. Clearly, the use of cisplatin as primary reference is beneficial in these cases, because the relativistic effects on the absolute shielding constants (see *Table 6*) are very similar for these closely related systems.

For the metal-coordinated N(3)-atom, the accord between computed and experimental coordination shifts improves when the spin–orbit effect is included. For instance, on going from ZORA to ZORA-SO, the deviation between theory and experiment for this nucleus decreases from *ca*. 55 to 33 ppm for **11**, and from *ca*. 50 to 36 ppm for **12**.

The reasons for these remaining discrepancies are not fully clear at the moment. According to the PCM results from the preceding section, solvation effects do not appear to be a major source for this error.

For the 4d complexes **6**–**10**, no experimental ^{15}N-NMR data are available for comparison. In light of the results for **11**/**12**, the predicted coordination shifts for N(3), *ca.*

– 57, – 48, – 71, and – 59 ppm for **6**, **7**, **9**, and **10**, respectively (ZORA-SO values from *Table 7*), are, in an absolute sense, probably lower limits. Whereas it is well-known that SO coupling has a significant effect on NMR properties of nuclei bonded to 5d elements such as Pt, Au, and Hg [38][78][92], the extent of this effect is also remarkable for the 4d complexes of this study. This result is significant for further computational work dealing with transition metal complexes of biological interest that contain different metals and coordination environments. Concerning the question whether nonrelativistic or scalar relativistic approaches are still useful for calculating $\delta(^{15}N)$ of N directly coordinated to a 4d metal such as Pd, Ru, and Rh, we now show that SO effects are also significant for these species. In this case, our findings can be rationalized by the large s-character of the metal–N bond with its sp^2-hybridized N-atom that allows for a particularly effective *Fermi*-contact interaction, thus producing a large SO coupling for the 5d complexes, and also to a notable one for the 4d species. Less pronounced effects are expected for ligands with weaker σ-donor capability or less s-character in the bond.

Complex **8** is rather large for a ZORA-SO calculation. To estimate the SO effects, we performed calculations on a smaller model complex $[Rh_2(OAc)_4(NCH)_2]$ (**15**) with HCN instead of dimetridazole (**1**) ligands (see *Fig. 3*). Because the metal–N bond has a larger s-character in **15** compared to that in the complex with **1**, the resulting SO effects on $\delta(^{15}N)$ and $\sigma(^{103}Rh)$ in the model should be upper limits for the actual effects in **8**. The scalar relativistic effects are deshielding by *ca.* 6 and – 150 ppm for $\delta(^{15}N)$ and $\sigma(^{103}Rh)$, respectively (compare δ(NREL) and δ(ZORA) values in *Fig. 3*)[2]). Similarly large, but shielding SO effects are found for both nuclei, *ca.* – 5 and 170 ppm for $\delta(^{15}N)$ and $\sigma(^{103}Rh)$, respectively (compare δ(ZORA) and δ(ZORA-SO) values in *Fig. 3*). Only small total relativistic corrections are, thus, predicted for $\Delta\delta(^{15}N)$ and $\delta(^{103}Rh)$ for **8**.

The SO effect on the ^{103}Rh shielding constant in **15** is noteworthy, but is relatively small, given that, in this complex, the metal itself is bonded to a heavier nucleus, namely the second Rh-atom. In previous theoretical studies of NMR parameters of systems

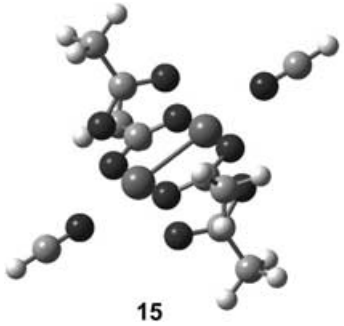

Method	$\delta(^{15}N)$	$\sigma(^{103}Rh)$
NREL/TZP	–141.4	–4880
ZORA/TZP'	–135.0	–5025
ZORA-SO/TZP'	–140.4	–4855

Fig. 3. *Structure of the model complex* **15** ($[Rh_2(OAc)_4(NCH)_2]$, *together with computed* ^{15}N*-NMR chemical shifts and* ^{103}Rh *magnetic-shielding constants obtained at non-relativistic, ZORA, and ZORA-SO levels.* Values in ppm.

[2]) Note the different sign convention for σ and δ: increased shielding manifests itself in an increased σ value, but in a decrease in the chemical shift, δ.

with metal–metal bonds, the computed values emerged as a delicate interplay between features of the metal–metal bond, relativistic effects, the influence of the ligands, and the influence of the solvent (this is seen, *e.g.*, in the case of Pt,Pt coupling constants, which can differ by a factor of 10 for chemically closely related dinuclear Pt complexes [93]). Assuming that the relativistic effects on $\sigma(^{103}\text{Rh})$ in the model system **15** is also transferable to the phosphite derivative **13**, only a small correction (which would only apply to this system, not to any mononuclear reference compound) of -25 ppm would result for the computed $\delta(^{103}\text{Rh})$ value (*vide infra*). The $\delta(^{99}\text{Ru})$ [94] and $\delta(^{103}\text{Rh})$ [95] values in larger sets of metal complexes have recently been studied with the ZORA method.

4. Conclusions. – We have presented a computational study of geometries and NMR chemical shifts of a number of transition-metal complexes with the dimetridazole (**1**) ligand. The chosen species are prototypical representatives of the large family of metal-nitro-1*H*-imidazole complexes, which are of interest due to their physiological properties and pharmacological relevance as potential radiosensitizers. In those cases where ^{1}H-, ^{14}N-, and ^{195}Pt-NMR data are available, the observed δ values or coordination shifts, $\Delta\delta$, are reasonably well reproduced at the GIAO-B3LYP or -BP86 levels employing BP86/ECP1 geometries, provided relativistic effects are taken into account. The latter have been included using the popular ZORA approach including spin–orbit (SO) coupling. SO Effects are particularly important for $\delta(^{15}\text{N})$ of the metal-coordinated N atom, where they can exceed 20 ppm. Relativity in particular can thus serve as a 'magnifying glass' for subtle changes in the electronic structure of metal–N bonds. Scalar relativistic and geometrical effects, as well as solvation effects modeled using a polarizable continuum method, are indicated to be of lesser importance in this case.

In those cases where not all chemical shifts have been reported yet, our computed values may serve as reliable predictions, which can be helpful as guidance for eventual experimental detection. This is especially true for the $\delta(^{103}\text{Rh})$ and $\delta(^{99}\text{Ru})$ values, which are indicated to be very sensitive NMR probes for the complexes under scrutiny, and which appear to be within reach of modern NMR techniques. Quantum-chemical calculations as those presented here can be a valuable ingredient in the study of metal-nitro-1*H*-imidazole complexes. Such calculations provide a better understanding of structure and bonding in these complexes, and complement multinuclear NMR spectroscopy as an important tool for their characterization in solution.

We are grateful to both Brazilian and German agencies, *CAPES* and *DAAD*, respectively, for funding part of this work. *M. B.* wishes to thank the *Deutsche Forschungsgemeinschaft* for a *Heisenberg* fellowship, and Prof. *W. Thiel* for continuous support. Finally, *J. D. F. V.* and *R. B. A.* wish to thank for the financial support provided by the Brazilian agencies FAPERJ and CNPq.

REFERENCES

[1] R. Benn, A. Rufinska, *Angew. Chem., Int. Ed.* **1986**, *25*, 861.
[2] P. S. Pregosin, 'Transitional Metal Nuclear Magnetic Resonance', Elsevier Amsterdam, 1991.
[3] W. von Philipsborn, *Chem. Soc. Rev.* **1999**, *28*, 95.
[4] 'Calculation of NMR and EPR Parameters. Theory and Applications', Eds. M. Kaupp, M. Bühl, V. G. Malkin, Wiley-VCH, Weinheim, 2004.

[5] T. Helgaker, M. Jszunski, K. Ruud, *Chem. Rev.* **1999**, *99*, 293.
[6] M. Bühl, F. T. Mauschick, F. Terstegen, B. Wrackmeyer, *Angew. Chem.*, *Int. Ed.* **2002**, *41*, 2312.
[7] J. M. Brown, B. G. Wouters, *Cancer Res.* **1999**, *59*, 1391.
[8] H. Horis, H. Nagasawa, in 'Advances in Environmental Science and Technology, Vol. 28: Environmental Oxidants', John Wiley & Sons, New York, 1994.
[9] H. Hori, C. Z. Jin, M. Kiyono, S. Kasai, M. Shimamura, S. Inayama, *Bioorg. Med. Chem.* **1997**, *5*, 591.
[10] J. D. Chapman, L. R. Coia, C. C. Stobe, E. L. Engelhart, M. C. Fenning, R. F. Schneider, *Br. J. Cancer* **1996**, *74*, S204.
[11] B. P. Espósito, R. Najjar, *Coord. Chem. Rev.* **2002**, *232*, 137.
[12] A. Nunn, K. Linder, H. W. Strauss, *Eur. J. Nucl. Med.* **1995**, *22*, 265.
[13] I. Ségalas, A. L. Beauchamp, *Can. J. Chem.* **1992**, *70*, 943.
[14] N. Farrell, 'Transition Metal Complexes as Drugs and Chemotherapeutic Agents', Kluwer Academic, Dordrecht, 1989, Chapt. 8, p. 183.
[15] H. Kusuoka, K. Hashimoto, K. Fukuchi, T. Nishimura, *J. Nucl. Med.* **1994**, *35*, 1371.
[16] R. B. Lauffer, *Chem. Rev.* **1987**, *87*, 901.
[17] C. J. Anderson, M. J. Welch, *Chem. Rev.* **1999**, *99*, 2219.
[18] C. L. McCoy, D. J. O. McIntyre, S. P. Robinson, E. O. Aboagye, J. R. Griffiths, *Br. J. Cancer* **1996**, *74*, S226.
[19] R. C. Urtasun, J. D. Chapman, J. A. Raleigh, A. J. Franko, C. J. Koch, *Int. J. Rad. Oncol.* **1986**, *12*, 1263.
[20] H. Ali, J. E. van Lier, *Chem. Rev.* **1999**, *99*, 2379.
[21] T. C. Ramalho, M. A. La-Scalea, R. B. de Alencastro, J. D. Figueroa-Villar, *Biophys. Chem.* **2004**, *110*, 267.
[22] T. C. Ramalho, E. F. F. Cunha, R. B. de Alencastro, *J. Theor. Comput. Chem.* **2004**, *3*, 1.
[23] T. C. Ramalho, E. F. F. Cunha, R. B. de Alencastro, *J. Phys.: Condens. Mater.* **2004**, *16*, 6159.
[24] T. C. Ramalho, M.Bühl, *Magn. Reson. Chem.* **2005**, 43, 139.
[25] T. C. Ramalho, J. D. Figueroa-Villar, T. L. C. Martins, *Magn. Reson. Chem.* **2003**, *41*, 983.
[26] K. Coutinho, S. Canuto, *Adv. Quantum Chem.* **1997**, *28*, 89.
[27] K. Coutinho, S. Canuto, *J. Chem. Phys.* **2000**, *113*, 9132.
[28] K.Coutinho, S. Canuto, M C. Zerner, *J. Chem. Phys.* **2000**, *112*, 9874.
[29] K.Coutinho, S. Canuto, *J. Mol. Struct. THEOCHEM* **2003**, *632*, 235.
[30] M. Bühl, in 'Calculation of NMR and EPR Parameters. Theory and Applications', Eds. M. Kaupp, M. Bühl , V. G. Malkin , Wiley-VCH, Weinheim, 2004, p. 421.
[31] M. Bühl, S. Gaemers, C. J. Elsevier, *Chem.–Eur. J.* **2000**, *6*, 3272.
[32] T. Ziegler, *Chem. Rev.* **1991**, *91*, 651.
[33] W. Koch, M. C. Holthausen, 'A Chemist's Guide to Density Functional Theory', Wiley-VCH, Weinheim, 2000.
[34] K. W. Zilm, J. C. Duchamp, in 'Nuclear Magnetic Shieldings and Molecular Structure', Ed. J. A. Tossel, NATO ASI Series C386, Kluwer, Dordrecht, 1993, pp. 315.
[35] G. Schreckenbach, S. K. Wolff, T. Ziegler, *J. Phys. Chem. A* **2000**, *104*, 8244.
[36] D. B. Chesnut, in 'Reviews in Computational Chemistry', Eds. K. B. Libkowitz, D. B. Boyd, VCH, New York, 1996, Vol. 8, p. 245.
[37] D. B. Chesnut, in 'Annual Reports on NMR Spectroscopy', Ed. G. A. Webb, Academic Press, New York, 1994, Vol. 29, p. 71.
[38] J. Autschbach in 'Calculation of NMR and ESR Parameters. Theory and Applications' Eds. M .Kaupp, M. Bühl, V. G. Malkin, Wiley-VCH, Weinheim, 2004, p. 227; J. Autschbach, T. Ziegler, in 'Calculation of NMR and ESR Parameters. Theory and Applications' Eds. M. Kaupp, M. Bühl, V. G. Malkin, Wiley-VCH, Weinheim, 2004, p. 249; J. Autschbach, *Structure Bonding* **2004**, *112*, 1.
[39] M. Bühl, M. Kaupp, V. G. Malkin, O. L. Malkina, *J. Comput. Chem.* **1999**, *20*, 91.
[40] a) A. D. Becke, *Phys. Rev. A.* **1988**, *38*, 3098; b) J. P. Perdew, *Phys. Rev. B* **1986**, *33*, 8822; c) J. P. Perdew, *Phys. Rev. B* **1986**, *34*, 7406.
[41] P. Fuentealba, H. Preuss, H. Stoll, L. v. Szentpaly, *Chem. Phys. Lett.* **1989**, *89*, 418.
[42] M. Kaupp, P. v. R. Schleyer, H. Stoll, H. Preuss, *J. Chem. Phys.* **1991**, *94*, 1360.
[43] F. D. Rochon, R. Melanson, N. Farrell, *Acta Crystallogr., Sect. C* **1993**, *49*, 1703.
[44] C. Anderson, A. L. Beauchamp, *Can. J. Chem.* **1995**, *73*, 471.
[45] N. Galvan-Tejada, S. Bernes, S. E. Castillo-Blum, H. Nöth, R. Vicente, N. Barba-Behrens, *J. Inorg. Biochem*. **2002**, *91*, 339.
[46] T. M. Dyson, E. C. Morrison, D. A. Tochter, L. D. Dale, D. I. Edwards, *Inorg. Chim. Acta* **1990**, *169*, 127.

[47] J. R. Bales, C. J. Coulson, D. W. Gilmour, M. A. Mazid, S. Neidle, R. Kuroda, B. J. Peart, C. A. Ramsden, P. J. Sadler, *J. Chem. Soc.*, *Chem. Commun*. **1985**, 432.
[48] R. Ditchfield, *Mol. Phys.* **1974**, *27*, 789; K. Wolinski, J. F. Hinton, P. Pulay, *J. Am. Chem. Soc.* **1990**, *112*, 8251; J. R. Cheeseman, G. W. Trucks, T. A. Keith, M. J. Frisch, *J. Chem. Phys.* **1996**, *104*, 5497.
[49] A. D. Becke, *J. Chem. Phys.* **1993**, *98*, 5648.
[50] W. Kutzelnigg, U. Fleischer, M. Schindler, 'NMR Basic Principles and Progress', Springer-Verlag, Berlin, 1990, Vol. 23, p. 165.
[51] S. Huzinaga, M. Klobukowski, *J. Mol. Struct.* **1988**, *167*, 1.
[52] T. M. Cances, B. Mennucci, J. Tomasi, *J. Chem. Phys*. **1997**, *107*, 3032.
[53] V. Barone, M. Cossi, J. Tomasi, *J. Comput. Chem.* **1998**, *19*, 404.
[54] M. Cossi, V. Barone, B. Mennucci, J. Tomasi, *Chem. Phys. Lett*. **1998**, *286*, 253.
[55] M. Cossi, G. Scalmani, N. Rega, V. Barone, *J. Chem. Phys* **2002**, *117*, 43.
[56] M. Orozco, F. J. Luque, *Chem. Rev.* **2000**, *100*, 4187.
[57] M. Cossi, O. Crescenzi, *J. Chem. Phys.* **2003**, *118*, 8863.
[58] M. J. Frisch, G. W. Trucks, H. B. Schlegel, G. E. Scuseria, M. A. Robb, J. R. Cheeseman, V. G. Zakrzewski, J. A. Montgomery Jr., R. E. Stratmann, J. C. Burant, S. Dapprich, J. M. Millam, A. D. Daniels, K. N. Kudin, M. C. Strain, O. Farkas, J. Tomasi, V. Barone, M. Cossi, R. Cammi, B. Mennucci, C. Pomelli, C. Adamo, S. Clifford, J. Ochterski, G. A. Petersson, P. Y. Ayala, Cui Q, K. Morokuma, P. Salvador, J. J. Dannenberg, D. K. Malick, A. D. Rabuck, K. Raghavachari, J. B. Foresman, J. Cioslowski, J. V. Ortiz, A. G. Baboul, B. B. Stefanov, G. Liu, A. Liashenko, P. Piskorz, I. Komaromi, R. Gomperts, R. L. Martin, D. J. Fox, T. Keith, M. A. Al-Laham, C. Y. Peng, A. Nanayakkara, M. Challacombe, B. Johnson, W. Chen, M. W. Wong, J. L. Andres, C. Gonzalez, M. Head-Gordon, E. S. Replogle, J. A. Pople, *Gaussian Inc.*, Pittsburgh PA, 2003.
[59] E. J. Baerends, D. E. Ellis, P. Ros, *Chem. Phys.* **1973**, *2*, 41.
[60] G. te Velde, E. J. Baerends, *J. Comput. Phys.* **1992**, *99*, 84.
[61] E. J. Baerends, P. M. Boerrigter, L. Cavallo, L. Deng, R. M. Dickson, D. E. Ellis, L. Fan, T. H. Fischer, C. Fonseca Guerra, S. J. A. van Gisbergen, J. A. Groeneveld, O. V. Gritsenko, F. E. Harris, P. van den Hoek, H. Jacobsen, G. van Kessel, F. Koostra, E. van Lenthe, P. V. Osinga, P. H. T. Philipsen, D. Post, C. C. Pye, W. Ravenek, P. Ros, P. R. T. Schipper, G. Schreckenbach, J. G. Snijders, M. Sola, D. Swerhone, G. te Velde, P. Vernooijs, L. Versluis, O. Visser, E. van Wezenbeek, G. Wiesenekker, S. K. Wolff, T. K. Woo, T. Ziegler, ADF 1999, Theoretical Chemistry, Vrije Universiteit, Amsterdam, The Netherlands, 1999.
[62] S. K Wolff, T. Ziegler, E. van Lenthe, E. J. Baerends, *J. Chem. Phys.* **1999**, *110*, 7689.
[63] E. van Lenthe, R. van Leeuwen, E. J. Baerends, J. G. Snijders, *Int. J. Quantum Chem.* **1996**, *57*, 281.
[64] R. R. Ernst, G. Bodenhausen, 'Principles of Nuclear Magnetic Resonance in One and Two Dimensions', Clarendon Press, Oxford, UK, 1987; G. E. Martin, A. S. Zektzer, 'Two-Dimensional NMR Methods for Establishing Molecular Connectivity', Wiley-VCH, New York, 1988.
[65] B. C. Chen, W. von Philipsborn, K. Nagarajan, *Helv. Chim. Acta* **1983**, *66*, 1537.
[66] F. M. Macdonald, P. J. Sadler, *Magn. Reson. Chem.* **1991**, 29, S52.
[67] T. G. Appleton, J. R. Hall, S. F. Ralph, *Inorg. Chem*. **1985**, *24*, 4685.
[68] R. W. Dykstra, A. M. Harrison, *J. Magn. Reson*. **1982**, *46*, 338; C. Brevard, P. Granger, *Inorg. Chem*. **1983**, *22*, 532.
[69] M. Bühl, *Chem. Phys. Lett.* **1997**, *267*, 251.
[70] S. Gaemers, J. van Slageren, C. M. O'Connor, J. G. Vos, R. Hage, C. J. Elsevier, *Organometallics* **1999**, *18*, 5238.
[71] M. A. O. Volland, P. Hofmann, *Helv. Chim. Acta* **2001**, *84*, 3456.
[72] M. Bühl, M. Hakansson, A. H. Mahmoudkhani, L. Öhrström, *Organometallics* **2000**, *19*, 5589.
[73] P. W. N. M. Van Leeuwen, C. Claver, 'Rhodium Catalyzed Hydroformylation', Kluwer Academic, Dordrecht, 2000; R. S. Dickson, 'Homogeneous Catalysis with Compounds of Rhodium and Iridium (Catalysis by Metal Complexes)', Vol. 8, Reidel, Dordrecht, 1985.
[74] P. Tsiveriotis, N. Hadjiliadis, *Coord. Chem. Rev.* **1999**, *192*,171.
[75] S. J. Lippard, J. M. Berg, 'Principles of Bioinorganic Chemistry', University Science Books, Mill Valley, CA, 1994.
[76] G. J. Martin, M. L. Martin, J.-P. Gouesnard, 'NMR Basic Principles and Progress', Vol. 18, Eds. P. Diehl, E. Fluck, R. Kosfeld, Springer-Verlag, Berlin, 1981.
[77] M. Witanowski, L. Stefaniak, G. A. Webb, *Ann. Rep. NMR Spectrosc.* **1992**, *25*, 1.
[78] T. M. Gilbert, T. Ziegler, *J. Phys. Chem. A* **1999**, *103*, 7535.
[79] E. B. Boyar, S. D. Robinson, *J. Chem. Soc., Dalton Trans.* **1985**, 629.

[80] D. Magieram, W. Baumann, I. S. Podkorytov, J. Omelanczuk, H. Duddek, *Eur. J. Inorg. Chem*. **2002**, 3253.
[81] G. G. Christoph, J. Halpern, G. P. Khare, Y. B. Koh, C. Romanoswski, *Inorg. Chem*. **1981**, *20*, 3029.
[82] M. Bühl, *Chem.–Eur. J.* **1999**, *5*, 3515.
[83] C. Anderson, A. L. Beauchamp, *Inorg. Chem*. **1995**, *34*, 6065; I. R. Baird, S. J. Rettig, BvR. James, K. A. Skov, *Can. J. Chem*. **1998**, *76*, 1379.
[84] C. Anderson, A. L. Beauchamp, *Inorg. Chim. Acta* **1995**, *233*, 33.
[85] M. Bühl, P. Imhof, M. Repisky, *ChemPhysChem* **2004**, *5*, 410.
[86] S. Grigoleit, M. Bühl, *Chem.–Eur. J.* **2004**, *10*, 5541.
[87] R. Cammi, B. Mennucci, J. Tomasi, *J. Chem. Phys.* **1999**,*110*, 7627.
[88] K. V. Mikkelsen, K. Ruud, T. Helgaker, *J. Comput. Chem.* **1999**, *20*, 1281.
[89] M. Kaupp, V. G. Malkin, O. L. Malkina, D. R. Salahub, *Chem. Phys. Lett.* **1995**, *235*, 382.
[90] M. Kaupp, V. G. Malkin, O. L. Malkina, D. R. Salahub, *J. Am. Chem. Soc.* **1995**, *117*, 1851.
[91] M. Kaupp, O. L. Malkina, V. G. Malkin, P. Pyykkö, *Eur. J. Chem*. **1998**, *4*, 118.
[92] G. Schreckenbach, S. K. Wolff, T. Ziegler, *J. Phys. Chem. A* **2000**, *104*, 8244.
[93] J. Autschbach, C. D. Igna, T. Ziegler, *J. Am. Chem. Soc.* **2003**, *125*, 1028.
[94] A. Bagno, M. Bonchio, *Magn. Reson. Chem*. **2004**, *42*, S79.
[95] L. Orian, A. Bisello, S. Santi, *Chem.–Eur. J.* **2004**, *10*, 4029.

Received May 24, 2005